Volume 5
Number 10
October 2025
Pages 1065–1174

Environmental Science
Atmospheres

rsc.li/esatmospheres

ISSN 2634-3606

ROYAL SOCIETY OF CHEMISTRY

PAPER
Luke P. Harrison *et al.*
Effervescent nozzle design to enable outdoor marine cloud brightening experimentation

Environmental Science: Atmospheres

ROYAL SOCIETY OF CHEMISTRY

PAPER

View Article Online
View Journal | View Issue

Cite this: *Environ. Sci.: Atmos.*, 2025, **5**, 1071

Effervescent nozzle design to enable outdoor marine cloud brightening experimentation

Luke P. Harrison, *[ab] Chris Medcraft [b] and Daniel P. Harrison [bc]

Marine Cloud Brightening (MCB) is a proposed solar radiation management technique whereby the albedo of low-lying clouds is artificially enhanced by the addition of Cloud Condensation Nuclei (CCN). It is generally accepted that these would be produced by atomisation of seawater to produce droplets which form appropriately sized artificial sea spray aerosol (SSA). Despite extensive theoretical consideration of the MCB concept, progress in understanding how perturbations to complex cloud microphysical processes would evolve has been hampered by the technical inability to produce the very large numbers of SSA required. To facilitate the first phase of outdoor experimentation a single MCB station should be capable of producing around 10^{15} per s CCN. Effervescent nozzle technology has been posited as potentially capable of meeting these requirements. Here we describe an effervescent nozzle design that produces ~1.73×10^{12} per s SSA, with ~71% of aerosols within a 30 to 1000 nm range (considered likely CCN), using ~512 W of energy per nozzle. Producing 10^{15} CCN using this design would then require 814 nozzles and around 417 kW of energy, a demand that can be practically met on a research vessel. The nozzle described here is therefore sufficiently practical to facilitate outdoor *in situ* experimentation of MCB, enabling a new generation of perturbation experiments that directly probe cloud microphysical and radiative responses to aerosol.

Received 24th June 2025
Accepted 18th August 2025

DOI: 10.1039/d5ea00073d

rsc.li/esatmospheres

Environmental significance

Marine cloud brightening is a solar radiation management technique that is being considered for the protection of ecosystems, through either global or regional application, including over the Great Barrier Reef. Despite over 30 years of theoretical research, outdoor field experimentation could not proceed until technology was developed which could produce the required quadrillions per second of nano-sized sea salt crystals from seawater. In this submission we describe the development and laboratory characterisation of the dual fluid effervescent seawater atomising nozzle which was the technological development that has enabled the world's first outdoor field trials of MCB to be undertaken within the Great Barrier Reef.

1 Introduction

Marine Cloud Brightening (MCB) is one of several proposed solar radiation management techniques with the goal of reducing temperature rises associated with global climate change.[1,2] The technique aims to increase the number of available Cloud Condensation Nuclei (CCN) within susceptible low-lying marine clouds by providing sub micrometer sized sea salt aerosols, the activation of the additional CCN can increase cloud albedo.[3] Increased cloud albedo would reduce the amount of shortwave solar radiation reaching the sea surface, reducing surface temperature.[4] The concept was first advanced over three decades ago and there has been progress on understanding the theoretical implications of perturbing clouds in this manner through modelling studies[3,5,6] and the study of natural analogues.[7–9] However, practical demonstration of the concept and real-world experimentation to test theoretical work on cloud microphysical and radiative responses have been hampered by a lack of technology that can generate the very large numbers of nano sized sea salt aerosols required.[10]

Ambient aerosol concentrations in the marine boundary layer in remote ocean regions are typically low, resulting in low CCN concentrations of approximately 50 to 100 cm^{-3}. To produce a globally averaged negative forcing of ~−4 W m^{-2}, a target aerosol concentration increase of 200 to 400 CCN per cm^3 has been suggested for regions with the most susceptible clouds.[1] Such a change in radiative forcing would offset the expected temperature increase resulting from a doubling of carbon dioxide concentrations in the atmosphere,[11] currently expected by the year 2100.[12] Spraying of sub micrometer sized droplets of seawater at or near surface level has been proposed as the most efficient and practical method to produce the necessary CCN.[13] This technique would rely upon turbulent mixing and convection within the boundary layer to transport

[a]*School of Aerospace, Mechanical and Mechatronic Engineering, University of Sydney, 2006, Australia*

[b]*Reefs and Oceans Research Cluster, National Marine Science Centre, Southern Cross University, Coffs Harbour, 2450, Australia*

[c]*School of Geosciences, University of Sydney, 2006, Australia*

the resulting sea salt aerosols to the base of the clouds to be ingested and activated as CCN to form cloud droplets. Latham *et al.* suggests that for experimentally proving the MCB concept a "phase 1" spraying station should be capable of creating a measurable increase in cloud albedo at ~100 km downwind, which would require CCN production rates of between 10^{15} and 10^{16} particles per second.[11,13] Estimates of ideal production rates per station for implementation also vary over at least an order of magnitude from 10^{16} to 10^{17} s^{-1}.[1,6,13–15]

A major challenge to the technological implementation of MCB is producing particles within a size range optimized both for energy consumption and for tendency to activate as CCN. Early literature on MCB suggested sizes of 200 nm dry aerosol diameter.[13] Latham *et al.* found from an aerosol-cloud and precipitation interactions model (ACPIM) that salt particles with a mass greater than 3×10^{-19} kg (~33 nm dry sphere diameter) are large enough to significantly enhance the albedo. Connolloy *et al.*[35] 2014 sought to include the assumed energy required to produce the sea spray into an optimization of the ideal droplet size. They employed a cloud parcel model to explore the effect that altering the aerosol particle size distribution has on the activation and growth of drops while assuming energy for droplet production was proportional to the water volume spraying rate. They concluded that particles with diameters from 30 to 100 nm were optimal in terms of energy efficiency for MCB, showing essentially that the proportion of the artificially produced aerosol population that successfully activates decreases less rapidly than the volume of water sprayed in this size range. Given that aerosol size dependent microphysical responses for *in situ* MCB cloud perturbation experiments using sea salt aerosol have not yet been reported, the ideal size distribution for MCB remains uncertain.

Effervescent atomization is a twin fluid atomization technique which uses a mixture of high-pressure liquid and gas to produce remarkably small droplets in relation to injection pressures and orifice size.[16] The technology relies on the gas, in this case air, being introduced into the flowing liquid (seawater) to create a bubbly two-phase flow. As the liquid exits the orifice it breaks into ligaments, which are then shattered into fine droplets by the rapid expansion of the gas.[17] Cooper *et al.* investigated the use of effervescent technology for MCB sea spray generation and estimated that their nozzle configuration could produce 5.3×10^{12} particles per second, with a count median diameter (CMD) of 63 nm using 0.43 mL per s saline solution. This conclusion assumed that the size distribution of aerosol produced could be adequately approximated with a log-normal distribution. However the reported experimental results showed that the tail did not follow a log-normal distribution.[18] A long 'tail' consisting of a small number of larger sized particles, can account for the majority of the liquid mass flow, due to the cube relationship between diameter and volume and thereby lead to an overestimate of the production rate. This was the case in the results reported by Cooper *et al.* due to a flaw in the methodology as the experiments reported here reveal.

The original objective of the present work was to confirm the performance of the effervescent nozzle design of Cooper *et al.*[18] and to explore the feasibility of upscaling to a system of sufficient scale that could be operated from a research vessel to enable initial insitu experimentation on cloud. For this we adopted a design energy goal of around 100–200 kW, being a quantity of energy that can be practically provided on a modestly sized research vessel and target production rate of around 10^{15} s^{-1}. In order to reach the target specification an improved nozzle configuration was developed and is described here along with an improved methodology for nozzle testing that is not subject to the previous errors in estimates of production rate and which also provides less biased estimates of resulting sea salt aerosol size distributions.

2 Methods

2.1 Apparatus design

An experimental apparatus was developed to provide the air and seawater at a range of pressure and flow rates to facilitate testing of a variety of effervescent nozzle configurations. The basic principle of the apparatus and nozzle arrangement follow that described by Cooper *et al.*[18] To simplify the experimental equipment required, pressurized air over water, contained within a pressure vessel was used to pressurize the water flow rather than the use of a continuous piston displacement pump. This difference means that the present apparatus runs in a batch mode with a maximum discrete run time determined by the volume of water in the pressure vessel and the water flow discharge rate. It has the advantage of operating smoothly without the need to dampen the flow fluctuations introduced by the high-pressure water pump. It also has the advantage of allowing the testing of a wider range of flow rates without requiring a set of pumps of multiple specification. The flow rate maximum is limited by the time requirement to obtain steady flow and time required to make sufficient measurements. A disadvantage is that the nozzle can not be run over long periods of time to test for degradation in performance characteristics. The supply of high-pressure air was never limiting in these experiments.

The apparatus consists of a water reservoir, air pressure supply SCUBA tank, 1/4″ and 1/16″ stainless steel tubing and various valves and pressure regulators (Fig. 1b). The pressure supply is regulated, and airflow passes a 20 μm filter before being used to pressurise the water reservoir and supply the gas for the effervescent nozzle. The filtered seawater is preloaded into the pressure vessel which is arranged vertically such that pressurized air, introduced to the upper portion, sits above the water which exits at the bottom of the vessel. During spraying operation, the liquid exits the pressure vessel through a 20 μm filter, followed by impedance tubing, formed of a 30 cm length of 1/16″ tubing with a 374 μm bore, to enter the bottom of the mixing tee. The mixing chamber used in this study is a modified post column reaction tee from Valco Instruments Ltd, as described in the Cooper *et al.* study. Air is supplied to the rear of the mixing tee through 1/4″ stainless tubing and water supplied to the side/bottom of the tee through the flow impedance tubing. Both the air and water flow rates were monitored using Keller differential pressure transmitters (PD-33X). A control system allowed for real-time monitoring and control of flow

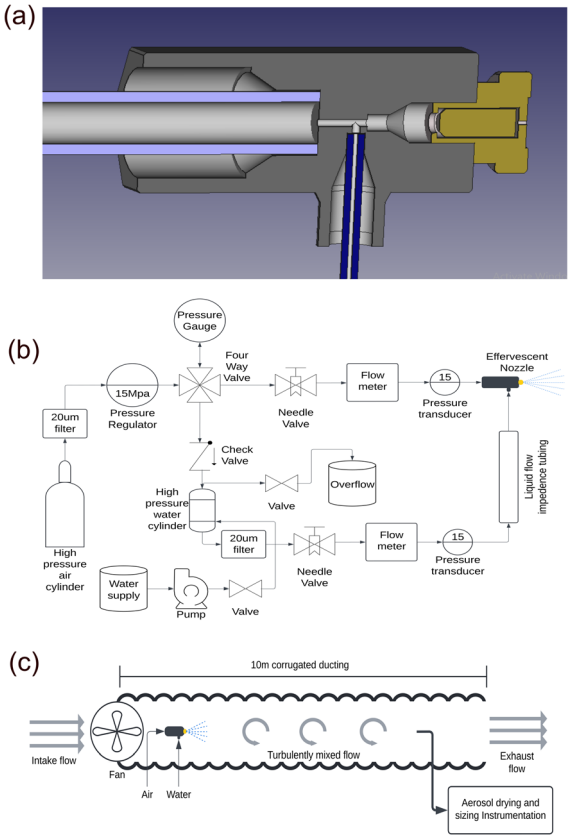

Fig. 1 (a) Digital model of the improved mixing tee and misting nozzle assembly with an internal divergence. Compressed air entering from the left of the mixing tee and seawater entering from the bottom through flow impedance tubing. (b) Schematic of the experimental effervescent nozzle flow/pressure supply. (c) Schematic of the wind tunnel/sampling experimental design.

rates and Gas to Liquid Radios (GLR). A schematic of the apparatus design, including all major components is shown in Fig. 1b.

Comparison tests were initially conducted using the configuration and geometry as described within the Cooper *et al.* study.[18] Numerous variations to the nozzle geometry and operating parameters were then explored in an effort to improve aerosol production rate and efficiency (number production rate per unit energy). We do not report here the many iterations, but rather report the results of what we found to be the optimum arrangement of those tested. Notable alterations included the replacement of the sapphire exit orifice with a commercial 'misting' nozzle (MT.201SS, Tecpro Australia) which includes an internal divergence before a 200 μm exit orifice. Another change was an increase from 250 to 750 μm internal bore size for both the gas and liquid entry orifices to the mixing tee. The internal divergence is used in misting nozzles to create a spray pattern when operating with solely liquid. Results are presented for the updated nozzle arrangement (750 μm internal bore size) and for the 250 μm internal bore size, as used in the Cooper *et al.* study, to illustrate their respective contributions to the improvement in production rate achieved by this work. The internal configuration of the mixing tee and commercial misting nozzle are shown in Fig. 1a, with gas entering from the left and liquid entering from below.

The experiments used filtered seawater from the supply at the National Marine Science Centre (NMSC), Southern Cross University, located in Charlesworth Bay, Coffs Harbour (Lat −30.266705°, Lon 153.140628°). The NMSC uses a flow through seawater supply system, taking water from Charlesworth Bay before filtration to 5 μm and UV sterilisation. The salinity of the water used in the present experiments was 29.4 ppt.

2.2 Sampling methodology

A schematic of the sampling design is shown in Fig. 1c. Characterization of the produced aerosol was undertaken subsequent to passage along a small portable wind tunnel, 10 m long by 0.6 m in diameter with wind speeds from 5 to 6 m s^{-1}. Aerosol measurement instrumentation was placed approximately 9 m downwind of the nozzle outside the wind tunnel, with a sampling probe extended into the tunnel at a 90° angle to extract sample air. Two (700 mm and 400 mm long) Nafion dryers (Perma Pure, USA) were used in series to dry the sample flow for all instrumentation. An aerosol dilutor (DI-1000, Dekati, Finland) was placed in line to reduce the total aerosol concentration. The dilution amount was measured before each test and then applied to the subsequent nozzle test. Aerosol sampling instruments included two Brechtel 1720 Mixing Condensation Particle Counter (MCPC), a Brechtel 2100 Scanning Electrical Mobility Sizer (SEMS) and a TSI 3321 Aerodynamic Particle Sizer (APS). Together the SEMS and APS measure aerosols with diameters ranging from 0.01 to 10 μm (10 to 10 000 nm). Simultaneous measurements were taken with both instruments and then processed using R Software.[19] The aerodynamic particle size, as measured by the APS, was converted to volumetric particle diameter with an assumed particle composition of NaCl (1.3 g cm^{-3} at 50% RH).[20] The SEMS and APS size distributions were joined by averaging the particle concentrations within the instrument overlap region (~524–1000 nm). The aerosol size distribution as measured by the SEMS and APS was then scaled by total concentration to match that of the MCPC. The sample line relative humidity was measured at the inlet of the SEMS and used to correct the particle diameter to dry diameter, if necessary, *i.e.* if the relative humidity was above 50%. The resultant size distribution was then corrected for inlet losses using the particle loss calculator.[21] The ambient size distribution and number concentration was measured and subtracted from the test. Background concentrations ranged from 3740 to 35 755 cm^{-3}, representing approximately 0.5–3% of the aerosol concentrations measured during spraying tests.

To consider the potential effect of coalescence on particle size in previously reported studies, a spraying experiment was also conducted in a static volume of air contained within a gazebo of 40 m^3 volume. In this case the ambient concentration was reduced by recirculating the air within the volume through a HEPA filtering system until the background concentration was less than 1000 cm^{-3}, or less than 1% of the test concentration. The effervescent nozzle was sprayed into the air

volume for a duration of 30 seconds, and the air volume mixed with a large fan for 3 minutes from the commencement of spraying. In these experiments aerosol measurement was performed continuously for 30 minutes following the nozzle spraying commencement and using the same instrumentation as in the flow through wind tunnel experiments. Data analysis followed the same methodology as described above for the wind tunnel experiments however no diluter was used.

2.3 Lognormal fitting

A lognormal model was fitted to the size distribution data for use in production rate estimates, to match the methods described in the Cooper *et al.* study.[18] This was done using the nls (Nonlinear Least Squares) function of the 'stats' library of R, version 4.2.1.[19] The fitted log normal distribution (using 'dlnorm' command) has a density:

$$f(x) = 1/(\sqrt{(2\pi)}\ \sigma\ x)\ \mathrm{e}^{-((\log x\ -\ \mu)^2/(2\sigma^2))}$$

where μ and σ are the mean and standard deviation of the logarithm. The mean is $E(X) = \exp(\mu + 1/2\ \sigma^2)$, the median is $\mathrm{med}(X) = \exp(\mu)$, and the variance $\mathrm{Var}(X) = \exp(2 \times \mu + \sigma^2) \times (\exp(\sigma^2) - 1)$ and hence the coefficient of variation is $\mathrm{sqrt}(\exp(\sigma^2) - 1)$ which is approximately σ when that is small (*e.g.*, $\sigma < 1/2$).

2.4 Volume calculations

To convert the measured dry particle diameter/number into sprayed droplet volume, the particle diameter was multiplied by 4.1 to give the sprayed droplet diameter. This 4-fold reduction in diameter approximation from droplet to particle is based on a simple calculation of the diameter of a sphere with 3.0% (derived from measured salinity) mass of a given droplet, considering the density of seawater (1.03 g cm^{-3}) and the density of NaCl (2.16 g cm^{-3}). From the sprayed droplet diameter we could calculate the volume of an individual droplet at each size, and then proportionally apply that to the number concentration at each size.

2.5 Particle production rate

Two methods of calculating the total number of particles produced per second were employed, the first 'mass conservation' method replicated the approach of the Cooper *et al.* study, in which the total volume of sprayed liquid is apportioned according to the measured resultant size distribution, accounting for an assumed 4-fold reduction in diameter from droplet to dry salt particle.[18]

The second 'tunnel flux' method is introduced in this study. The spray is introduced within a wind tunnel of known diameter and measured wind velocity. The number production rate is then simply estimated as the flux of aerosols along the tunnel. Number concentration of aerosols per unit volume (# cm^{-3}), as measured by the MCPC, is multiplied by the calculated volume flux of air through the wind tunnel.

This estimate relies on the following assumptions,

(1) That the plume is evenly distributed by turbulent mixing across the cross sectional area of the wind tunnel, which was confirmed by taking measurements across the diameter of the tunnel.

(2) That there is no deposition of aerosol along the length of the wind tunnel. There is some deposition evidenced by accumulation of salt crystals on the interior tunnel walls following prolonged use of the tunnel. However, it is considered negligible as measurements taken at various distances along the tunnel for a consistent spray showed no discernible drop in number concentration with distance downwind.

2.6 Energy calculations

The theoretical energy required to compress the gas component of the flow was calculated for a scaled-up spraying system using eqn (1). The power requirement to compress air to a given pressure is calculated, adapted from Perry 1950 (ref. 22) (eqn (10)–(74a)):

$$P_{\mathrm{a}} = \frac{k \times ZWRT_1}{k-1} \times \left[\left(\frac{P_2}{P_1} \right)^{\frac{(k-1)}{k}} - 1 \right] \quad (1)$$

where P_{a} = power requirement for air, W; k = gas isentropic coefficient, $k = 1.4$; Z = gas compressibility factor, $Z = 1$; W = mass flow, kg s^{-1}; R = gas constant, J $(\mathrm{kg \cdot K})^{-1}$ = 8314/molecular weight, $R = 286.69$; T_1 = inlet gas temperature, K; P_1 = absolute inlet pressure, kPa; and P_2 = absolute discharge pressure, kPa.

The theoretical energy required to compress the liquid component of the flow was calculated for a scaled-up spraying system using eqn (2). The power calculation for liquid flow pressurisation is adapted from Douglas 2005 (ref. 23) (eqn (24.15)):

$$P_{\mathrm{w}} = \frac{P \times Q_{\mathrm{l}}}{600} \quad (2)$$

where P_{w} = power requirement for water, kW; P = pressure, Bar; Q_{l} = liquid flow rate, L min^{-1}.

3 Results

Initially the nozzle described by Cooper *et al.*[18] was replicated and tested using the spray apparatus and wind tunnel as described above. The resulting dry particle distribution (Fig. 2B) exhibited a (dN) mode diameter of 34.7 nm with a Count Median Diameter (CMD) of 46.6 nm and a Geometric Standard Deviation (GSD) of 1.93. Fig. 2b displays the dNd log dX along with standard error bars, with $n = 13$ samples. This distribution displays a smaller peak than that described in Cooper *et al.* (Fig. 2a). Additionally, the production rate measured in this study using the more direct 'tunnel flux' method was lower by around half an order of magnitude than that published in the Cooper *et al.* study. The tunnel flux estimate of total particle production rate used in this study resulted in 1.07×10^{12} s^{-1} compared with estimates of 3×10^{12} and 5.3×10^{12} in the

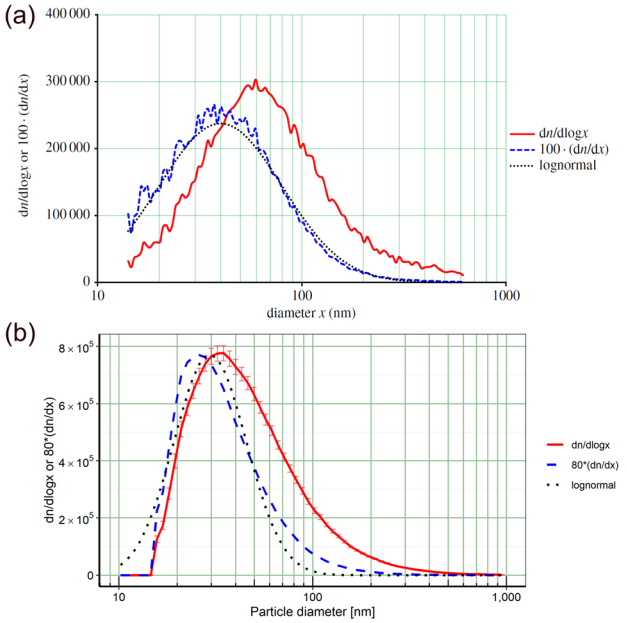

Fig. 2 Comparison of resulting size distribution of aerosol size, (a) as reported in Cooper *et al.*[18] and (b) tests undertaken with the same nozzle configuration during this study.

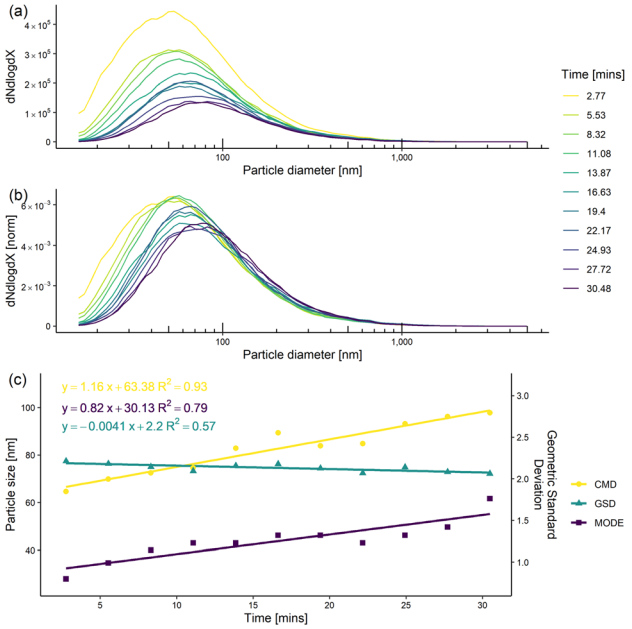

Fig. 3 Effects of coalescence on particle size characteristics over time in an enclosed air volume as used in previous studies. (a) Aerosol particle size distribution. (b) Frequency histogram of particle size normalised such that the integral over the density is equal to 1. (c) CMD, GSD and Mode changes over time for each scan, with solid lines showing a linear fit to each dataset.

Cooper *et al.* study, a difference of a factor of up to around 3 to 5 times.

The production rate was also estimated using the mass conservation method as used by the Cooper *et al.* study. Both the dry particle distribution (dN) and the lognormal fit of this data were used to calculate two separate production rate estimates, lognormal fitting is discussed in the methodology. Utilizing the measured distribution produced (dN) an estimate of total production rate of 3.49×10^{12} s^{-1} and using the lognormal distribution of dN/dX the production rate estimate was 2.06×10^{14} s^{-1}.

Experimentation was additionally carried out in a non-flow-through air volume (within a room), as performed within the Cooper *et al.* study.[18] Particle size distributions were measured continuously, with the SEMS performing a 1 minute long scan every ~2.75 minutes. Both the CMD and Mode increased over the course of measurement from 64.7 nm to 97.8 nm and 27.9 nm to 61.6 nm respectively, as shown Fig. 3c. The CMD and Mode increased at a relatively similar rate of 1.16 and 0.82 nm min^{-1} respectively. The total concentration of the first scan, important for estimating the rate of coalescence, was 1.1×10^5 cm^{-3}.

Various modifications to the effervescent nozzle configuration were trialled with the aim of increasing the production rate of the effervescent nozzle. The internal bore diameters (air and water inlets) were increased from 250 μm, as specified by Cooper *et al.*, to 750 μm, and the nozzle orifice was increased from 150 μm to 200 μm.[18] Additionally, the pressure was increased from 9 MPa in Cooper *et al.* to 15 MPa and the GLR varied between 0.374 to 1.0. These changes in aggregate contributed to an increase in total production rate from 1.07×10^{12} s^{-1} to 1.73×10^{12} s^{-1}, as measured in the present study using the tunnel flux method (Fig. 4a). Interestingly, there is

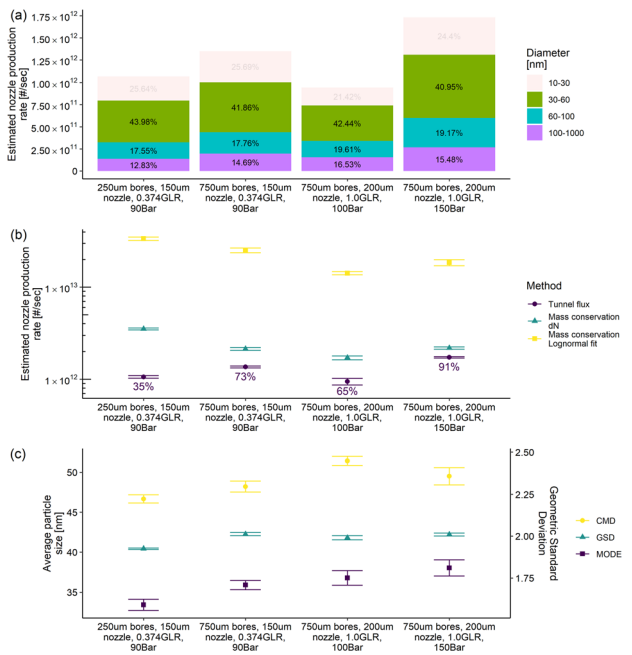

Fig. 4 (a) Size apportioned production rate estimates from the tunnel flux method for the modified nozzle fitted with a commercial misting orifice across a range of iterations in operating pressure, GLR, bore size, and orifice size. The bar graph labelling indicates the fraction of each size range (dry aerosol diameter) to the production rate estimate. (b) Production rate estimates comparing the three methodologies used. Percentages denote the percentage mass closure achieved. Note the log Y axis. (c) The particle sizing statistics for the total distributions.

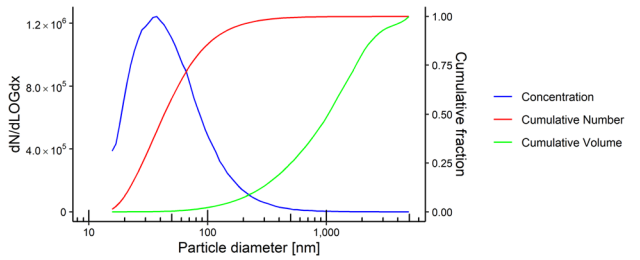

Fig. 5 Particle size distribution and cumulative volume and particle count for highest production rate nozzle.

little change in the CMD and the Mode of the particle size distribution with increasing pressures and GLRs (Fig. 4c).

The estimates of total production rate derived from the mass conservation method were higher than that of the tunnel flux estimate, by a factor of up to around 3.3× (Fig. 4b). Estimates using the conservation of mass method with lognormal assumption were higher still, by a factor of up to around 31.8×. The salt mass closure of each nozzle configuration, *i.e.* the cumulative measured salt *vs.* the theoretical amount of salt emitted by each nozzle varied significantly. Mass closure of 91% was achieved for the final nozzle version whereas only 35% was achieved for our replica Cooper *et al.* nozzle.[18] The dry particle size distribution remained remarkably consistent across all variations of the effervescent nozzle tested, including altering the orifice diameter, salt concentration, GLR and input pressure. The size distribution of the highest production rate nozzle tested, shown in Fig. 5, had a CMD of 49.5 nm dry particle diameter and a GSD of 2.01. This nozzle was configured with 750 μm bores for both air and water, a 200 μm nozzle orifice and was operated at 1.0 GLR and 15 MPa. For this nozzle ~94% of sea salt aerosol were below 200 nm dry diameter, however this 94% number fraction accounts for only 7.1% of the total volume of water sprayed. This nozzle produces an estimated 1.73×10^{12} s^{-1} droplets from 0.41 mL s^{-1} filtered seawater (and 0.3 L s^{-1} of air) with 71% of those particles being within the assumed MCB effectiveness range of 30 to 1000 nm dry diameter.

To reach a target CCN production rate of 10^{15} s^{-1} within the 30–1000 nm size range would require 814 of this current effervescent nozzle. An air compressor with an assumed efficiency of 0.72 could produce the required 14.7 m^3 min^{-1} (0.3 L s^{-1} × 814 nozzles) of air compressed to 15 MPa using an estimated 410.7 kW of power (eqn (1)). The required 20 L min^{-1} (0.41 mL s^{-1} × 814 nozzles) of seawater pressurised to 15 MPa could be supplied by a standard water pump and would only require 6.7 kW assuming a pump efficiency of 0.75 (eqn (2)). Combined this spraying equipment would require 417.4 kW to supply the 814 nozzles.

4 Discussion and conclusions

Study of the viability of the MCB technique either regionally or globally, requires the design and construction of MCB seawater sprayer equipment to enable outdoor cloud perturbation experiments to commence. The nozzle design described here and its robust characterisation were instrumental in the design and construction of the world's first prototype MCB equipment, the Aerosol, Radiation, and their Interactions Experimental Laboratory (ARIEL).[24] Equipped with the effervescent nozzle described here, a prototype of 100 nozzles requiring approximately 55 kW facilitated the initial outdoor tests undertaken by Harrison *et al.*[25] and originally suggested by Latham *et al.*[1] Latham *et al.*[1] suggested an initial 'phase 1' field campaign aimed at measuring the near field evolution of a sea salt aerosol plume in the marine boundary layer which was undertaken in 2020 by Southern Cross University and partners using the 100 nozzle iteration of ARIEL.[26] Key questions which can be assessed during these early stage outdoor experimental testing of MCB spraying equipment using the nozzle technology described here include the number production rate, effect of coalescence from multiple closely spaced nozzles on the resulting particle size distribution and how it evolves within the plume as it travels downwind, the dispersion of the plume within the marine boundary layer,[27] the physical and chemical characteristics of the sea spray aerosol produced and the ability of the spray generation equipment to operate robustly and continuously at sea for the necessary periods.

Further scaling up of the spraying system output is required to facilitate the following 'phase 2' stage of outdoor field testing suggested by Latham *et al.*,[1] involving characterising the dispersion of an MCB plume and its interaction with cloud microphysical processes. This work is currently being undertaken using an upgraded version of ARIEL that consists of 640 of the effervescent nozzles described here. Hernandez *et al.*[28] report initial results from these sea trials showing that the aerosol plume generated was able to raise the concentration of CCN at cloud base height by 1.25× with the vessel at anchor. The following phases of experimentation into MCB require detailed aircraft collected measurements[29] of cloud microphysical properties and how they change as a result of the sea salt aerosol injection. This work is currently underway within the Reef Restoration and Adaptation Program Cooling and Shading Subprogram (RRAP-CS), exploring the sensitivity of trade wind cumulus clouds over the Great Barrier Reef Australia to MCB.[30–32] This program of outdoor atmospheric testing of Marine Cloud Brightening has the prospect to greatly enhance our understanding of cloud microphysical processes and susceptibility to possible Climate Change interventions.

Energy availability on research vessels is limited[33] and development of the ARIEL system to the necessary levels of output were facilitated by the performance improvements made to the original effervescent nozzle described in the Cooper *et al.* study.[18] Alterations to the mixing tee geometry and operating parameters led to an ~60% increase of the total particle production rate from 1.06×10^{12} s^{-1} to 1.73×10^{12} s^{-1} (Fig. 4) with the CMD increasing from 46 nm to 49.5 nm, with a GSD of 2.01. This increase in particle production rate and CMD equate to a 60% reduction in the number of nozzles required to facilitate outdoor experimentation of MCB. When Latham *et al.*[2] speculated on appropriate production rates for a single station for various stages of MCB experimental work he assumed a monomodal spay, however the effervescent technique

produces spray over a wide range of sizes from 10 to 500 nm dry diameter. There remains considerable debate in the literature about the ideal sea salt aerosol size for MCB as well as minimum and maximum suitable sizes.[34,35] Here we take the range of 30–1000 nm adopting the lower limit advocated by Connolly *et al.* and an upper limit of 1000 nm. Of the total aerosols produced by our nozzle 71% or 1.16×10^{12} s^{-1} are within the range of 30 to 1000 nm dry particle diameter, which we will hence forth assume as suitable to act as CCN. In reality this is a gross oversimplification because the actual fraction which will activate as cloud droplets is situationally dependent. Numerous factors determine the activated fraction of total aerosols within a cloud such as supersaturation, the background aerosol concentration, size distribution, hygroscopicity and other factors.[36,37] Based on the most conservative tunnel flux method the current version of ARIEL achieves 1.11×10^{15} s^{-1} total production rate, with 7.86×10^{14} s^{-1} within the target CCN range using 640 effervescent nozzles.

To achieve the target of 10^{15} per s CCN by the criteria above rather than 10^{15} s^{-1} total aerosol would require 814 of the current nozzles. We can consider the air, water, and energy requirements of such a system. With each nozzle requiring ~0.3 L s^{-1} uncompressed air per nozzle, this would equate to 14.7 m^3 min^{-1} of FAD compressed to 15 MPa, requiring 410.7 kW of energy. An additional 6.7 kW of energy would be required to compress the 0.41 mL s^{-1} per nozzle (20 L min^{-1} total) to the required 15 MPa. A total energy requirement of 417.4 kW would likely be attainable *via* a simple, albeit large, diesel generator for initial experimentation. However, further scaling up of this nozzle to reach a implementation production rate of 10^{16} would require approximately 4.2 MW of energy per station, which is unlikely to be easily attainable for deployment scenarios. Incrementally ramping up MCB field experimentation has been suggested to mitigate the potential for unforeseen consequences.[1,6]

In this study we used a more conservative method to measure the production rate of effervescent nozzles compared with the mass conservation method used by Cooper *et al.*[18] Our results highlight how the mass conservation method can lead to significant overestimation of production rate due to the disproportionate effect that large, difficult to sample, particles can have on the estimate. Larger particles are more prone to losses which lead to under sampling due to their increased likelihood of settling out, particularly in a stagnant sampling chamber environment or through momentum losses within aerosol instrumentation inlet tubing.[38] A further problem with the mass conservation method is that it relies on the assumption that the measured size distribution is accurate and has not changed since the spray exited the nozzle, due to either particle losses or coalescence. The use of a lognormal fit to the experimental data in a mass conservation estimate of particle production rate as has been previously employed can further exaggerate the overestimation. This can occur due to a failure of the log normal model to accurately describe the real size distribution, for example as Cooper *et al.* state "neglecting momentarily the very significant long tail at larger sizes, which is not lognormal". We note that the particular form of lognormal model fitted to the experimental data in Cooper *et al.* is not stated within their manuscript and therefore may not be directly comparable with that used in our study. Nevertheless, the extent to which the conservation of mass and lognormal assumptions can upwardly bias the estimation of number production rate, even using a tunnel, is evident from our results with the lognormal method.

The differences observed between the dry aerosol size distribution reported by Cooper *et al.*[18] and our replica nozzle (Fig. 2) can not been definitively resolved. Our apparatus differs in that the water supply is pressurised using gas over liquid, which introduces the potential for gas dissolution into the liquid supply. However, the identified and most likely cause for the discrepancy is that whilst we conducted our tests within a relatively high flow wind tunnel, with short residence time, Cooper *et al.* conducted their testing within a large room with a long residence time, which could have led to coalescence of the particles prior to measurement. The amount of time between spraying and sampling is not stated in Cooper *et al.*, nor the total concentration within the sampling room. We considered the potential implications of using an enclosed volume of receiving air in this study and found that the size distribution shifted continuously after spraying (Fig. 3). The aerosol concentration in the enclosed receiving volume at our first scan was 1.1×10^5 particles cm^{-3}, it is unknown how this compares to that of Cooper *et al.* After 12 minutes our measured dry particle size distribution mode had shifted from 30.1 nm to 39.98 nm (fitted line), which was close to that reported by Cooper *et al.* (40 nm mode). Thus, our results indicate that coalescence occurring over a delay in sampling an enclosed receiving air volume could account for the differences in particle size distributions produced by our replica nozzle and that of Cooper *et al.*

The experimental apparatus described here allows for real-time control of the pressures and GLR of the effervescent nozzle (Fig. 1b). However, there are some limitations to the 'batch' mode of operation. The maximum spray period is dictated by the volume of the supply pressure chamber and liquid flowrate of the nozzle under test. For higher flow nozzles this can become a hindrance to effective sampling given also the relatively long scanning period required for a reasonable bin resolution in most SMPS. Fast size scanning aerosol sizing instrumentation, such as the Differential Mobility Sizer DMS500 (Cambustion, UK)[39] can overcome this limitation to some extent, however suffer lower size resolution and have less sensitivity than SMPS.[40] Another potential disadvantage of our laboratory effervescent apparatus is the gas over liquid approach to pressurising the liquid supply. Using this technique removes the need for a high pressure water pump and impacts of pump pulsation, however there is the possibility of gas dissolving into the liquid, which, if it occurred may alter particle breakup dynamics during spraying. Our results suggest that in the case of effervescent spray any impact of dissolved gas on the resulting aerosols size distribution are negligible. When operated at the same GLR, results from the batch plant are indistinguishable from those produced by the ARIEL plant which runs continuously.

We assert that the methodology described in this study provides a reliable and conservative method of estimating nozzle particle production rate for testing various MCB nozzle designs. The use of a turbulently mixed wind tunnel with aerosol counting and sizing instrumentation supplied by an isokinetic sampling inlet positioned downwind allows for comparison between two particle production rate calculation methods for every measurement. The ability to conduct mass closure analysis between the mass of salt entering the nozzle and the mass of salt measured as resulting aerosol flux along the tunnel provides a substantial increase in confidence over previous methods.

Using the measured aerosol concentration and airflow in the tunnel to estimate particle production rate is conservative because it is subject to undercounting if losses occur to the tunnel walls or fallout. Fallout of larger particles is revealed through the mass closure procedure described. The method relies on the assumption that the tunnel is sufficiently turbulently mixed such that particle concentration is uniform across the diameter of the tunnel. We caution that the tunnel and operating wind speed should be designed to achieve an even distribution and measurements undertaken to confirm. Monitoring the spray continuously as it travels down the tunnel has the advantage of allowing the identification of fluctuating or non-uniform spraying performance.

Confining a high production rate spray within the wind tunnel at high concentrations may allow coalescence that would not occur in an unconfined area, such as a large scale deployment. However, the amount of coalescence should be fixed for a given nozzle and set of tunnel operating conditions (*e.g.* wind speed). The tunnel flux method is likely to slightly underestimate the total particle production rate of the nozzle due to these losses but forms a more reliable basis for engineering design of spraying systems. With great care the mass conservation method gives results within a factor of around 2, however is prone to large errors if aerosols resulting from all large droplet sizes are not representatively sampled. The log-normal fit method of estimating production rate should be discounted for size distributions that are not perfectly fitted by this model with particular attention being given to the tail of larger sized aerosols. In the case of effervescent spraying its use leads to unrealistic order of magnitude too high production rate estimates. Previous characterization of effervescent nozzles for MCB used a methodology of spraying into a large, contained volume of air to characterise resulting aerosol size distributions. Coalescence driven by the sustained high concentrations of aerosol contained within the volume of air can also lead to inaccurate aerosol sizing if measurements are not taken immediately.

The size distribution obtained from the modified effervescent nozzle is sufficient for preliminary field testing and development of the MCB concept with 71% of sea salt aerosols produced within the range of 30–1000 nm (Fig. 5). However, 30 nm is on the low side for activation diameter in many low marine clouds, such as trade wind cumulus over the Great Barrier Reef which likely have lower supersaturations[41] then the marine stratocumulus cloud decks more commonly associated with MCB.[1,5,11,42] The minimum size at which particles begin to activate as cloud droplets (activation diameter) is dependent on their composition and the clouds supersaturation. According to Köhler theory, 30 nm NaCl particles would activate in a cloud with a supersaturation of approximately 0.6, which is higher than conventionally estimated for stratocumulus clouds but commensurate with more recent estimations for marine stratus clouds generally.[43] In a warm trade wind cumulus regime, common over the Great Barrier Reef during summer this level of supersaturation could be expected only under exceptionally low aerosol background conditions.[44] Even for these cloud types, the argument of 30 nm as an efficient size relies largely on the assumption that energy required to generate the particles is proportional to their volume,[35] which we have not found to be the case with current technologies. The proportion of 'suitable' aerosols drops very rapidly as the lower bound is increased above 30 nm (Fig. 5). It is therefore desirable to increase the mode of the resulting aerosol size distribution and narrow it as well. During our experiments we varied operating conditions of the nozzle to examine the effect on size distribution. Altering the input pressures, GLR's, nozzle orifice diameter, internal mixing tee bore size and length of internal mixing, all resulted in negligible variation to the size distribution. We hypothesise that due to the relatively high GLRs at which the nozzle shows high production rate (0.5 to 1.5) other changes in nozzle geometry or operating parameters have little effect on the mechanisms of droplet breakup. This is supported by the work of Lefebvre *et al.*[45] who showed diminishing change in particle geometric mean diameter towards higher GLRs. Further investigation is required into alternate nozzle designs and operating conditions to achieve a more monodisperse distribution of aerosols with a larger size mode from effervescent seawater spray.

In conclusion, the effervescent nozzle design presented in this study is capable of producing 1.73×10^{12} s^{-1} sea salt aerosols operating at a GLR of 1.0, and pressure of 15 MPa. 71% of these sea salt aerosols are within the 30 to 1000 nm dry diameter range posited as useful for MCB purposes. This production rate and energy efficiency have proven sufficient to enable the first generation of outdoor research experimentation into marine cloud brightening to proceed, paving the way for real-world cloud perturbation studies. To scale research further beyond the current phase of outdoor experimentation, improvement in the aerosol size distribution produced is desirable, and improvement in the production rate per unit of energy necessary to keep energy requirements reasonable. Future research should be directed at optimising both the particle size and the energy efficiency for producing large quantities of appropriately sized sea salt aerosols using either effervescent or alternative seawater atomisation techniques.

Author contributions

LH and DH designed the experimental study. LH and CM carried out experimental nozzle testing and analysed the data. All authors contributed to writing the manuscript and approved the final version.

Conflicts of interest

There are no conflicts to declare.

Data availability

The data that support the findings of this study are openly available in "Dryad" at **https://doi.org/10.5061/dryad.0cfxpnwbg**.

Acknowledgements

This work was funded by the 'Boosting Coral Abundance on the Great Barrier Reef Challenge" jointly funded by the Queensland State and Australian federal governments. DPH was funded by a Myer Foundation Innovation Fellowship. We wish to thank the late professor Ian S. F. jones for his guidance and contribution to these experiments.

Notes and references

1 J. Latham, K. Bower, T. Choularton, H. Coe, P. Connolly, G. Cooper, T. Craft, J. Foster, A. Gadian, L. Galbraith, H. Iacovides, D. Johnston, B. Launder, B. Leslie, J. Meyer, A. Neukermans, B. Ormond, B. Parkes, P. Rasch, J. Rush, S. Salter, T. Stevenson, H. Wang, Q. Wang and R. Wood, Marine cloud brightening, *Philos. Trans. R. Soc., A*, 2012, **370**, 4217–4262.

2 J. Latham and M. Smith, Effect on global warming of wind-dependent aerosol generation at the ocean surface, *Nature*, 1990, **347**, 372–373.

3 F. Hoffmann and G. Feingold, Cloud Microphysical Implications for Marine Cloud Brightening: The Importance of the Seeded Particle Size Distribution, *J. Atmos. Sci.*, 2021, **78**, 3247–3262.

4 C. W. Stjern, H. Muri, L. Ahlm, O. Boucher, J. N. S. Cole, D. Ji, A. Jones, J. Haywood, B. Kravitz, A. Lenton, J. C. Moore, U. Niemeier, S. J. Phipps, H. Schmidt, S. Watanabe and J. E. Kristjánsson, Response to marine cloud brightening in a multi-model ensemble, *Atmos. Chem. Phys.*, 2018, **18**, 621–634.

5 L. Ahlm, A. Jones, C. W. Stjern, H. Muri, B. Kravitz and J. E. Kristjánsson, Marine cloud brightening – as effective without clouds, *Atmos. Chem. Phys.*, 2017, **17**, 13071–13087.

6 R. Wood, Assessing the potential efficacy of marine cloud brightening for cooling Earth using a simple heuristic model, *Atmos. Chem. Phys.*, 2021, **21**, 14507–14533.

7 Y. C. Chen, M. W. Christensen, L. Xue, A. Sorooshian, G. L. Stephens, R. M. Rasmussen and J. H. Seinfeld, Occurrence of lower cloud albedo in ship tracks, *Atmos. Chem. Phys.*, 2012, **12**, 8223–8235.

8 M. W. Christensen, K. Suzuki, B. Zambri and G. L. Stephens, Ship track observations of a reduced shortwave aerosol indirect effect in mixed-phase clouds, *Geophys. Res. Lett.*, 2014, **41**, 6970–6977.

9 M. S. Diamond, H. M. Director, R. Eastman, A. Possner and R. Wood, Substantial Cloud Brightening From Shipping in Subtropical Low Clouds, *AGU Adv.*, 2020, **1**(1), e2019AV000111.

10 M. S. Diamond, A. Gettelman, M. D. Lebsock, A. McComiskey, L. M. Russell, R. Wood and G. Feingold, Opinion: To assess marine cloud brightening's technical feasibility, we need to know what to study-and when to stop, *Proc. Natl. Acad. Sci. U. S. A.*, 2022, 119.

11 J. Latham, P. Rasch, C. C. Chen, L. Kettles, A. Gadian, A. Gettelman, H. Morrison, K. Bower and T. Choularton, Global temperature stabilization *via* controlled albedo enhancement of low-level maritime clouds, *Philos. Trans. R. Soc., A*, 2008, **366**, 3969–3987.

12 IPCC Climate Change, *The Physical Science Basis*, 2013.

13 S. Salter, G. Sortino and J. Latham, Sea-going hardware for the cloud albedo method of reversing global warming, *Philos. Trans. R. Soc., A*, 2008, **366**, 3989–4006.

14 G. Cooper, D. Johnston, J. Foster, L. Galbraith, A. Neukermans, R. Ormond, J. Rush and Q. Wang, A Review of Some Experimental Spray Methods for Marine Cloud Brightening, *Int. J. Geosci.*, 2013, **04**, 78–97.

15 J. Latham, A. Gadian, J. Fournier, B. Parkes, P. Wadhams and J. Chen, Marine cloud brightening: regional applications, *Philos. Trans. R. Soc., A*, 2014, **372**, 4217–4262.

16 S. D. Sovani, P. E. Sojka and A. H. Lefebvre, Effervescent atomization, *Prog. Energy Combust. Sci.*, 2001, **27**, 483–521.

17 D. A. Nguyen and M. J. Rhodes, Producing fine drops of water by twin-fluid atomisation, *Powder Technol.*, 1998, **99**, 285–292.

18 G. Cooper, J. Foster, L. Galbraith, S. Jain, A. Neukermans and B. Ormond, Preliminary results for salt aerosol production intended for marine cloud brightening, using effervescent spray atomization, *Philos. Trans. R. Soc., A*, 2014, **372**(2031), 20140055.

19 R Core Team, *R: A Language and Environment for Statistical Computing, R Foundation for Statistical Computing*, 2022, **https://www.R-project.org/**.

20 P. F. DeCarlo, J. G. Slowik, D. R. Worsnop, P. Davidovits and J. L. Jimenez, Particle morphology and density characterization by combined mobility and aerodynamic diameter measurements. Part 1: Theory, *Aerosol Sci. Technol.*, 2004, **38**, 1185–1205.

21 S. L. Von der Weiden, F. Drewnick and S. Borrmann, Particle Loss Calculator–a new software tool for the assessment of the performance of aerosol inlet systems, *Atmos. Meas. Tech.*, 2009, **2**, 479–494.

22 J. H. Perry, *Chemical Engineers' Handbook*, ACS Publications, 8th edn, 1950.

23 J. F. Douglas, J. M. Gasiorek, J. A. Swaffield and L. B. Jack, *Fluid Mechanics*, 5 edn, 2005.

24 D. P. Harrison, C. Lemckert, S. Fitzgerald, H. Hunt, F. Hoffman, Z. Ristovski, B. Miljevic, M. Woodhouse and J. Middleton, *Marine Cloud Brightening in a Complex World – Moving beyond the Twomey Effect. Proposal to the Advanced Research + Invention Agency: Exploring Climate Cooling Programme*, Southern Cross University, 2025.

25 D. P. Harrison, L. Harrison, L. Cravigan and B. Kelaher, *Marine Cloud Brightening Proof Concept Study: Boosting*

Coral Abundance on the Great Barrier Reef Challenge (Final Report), Sydney Institute of Marine Science, Australia, 2020.

26 D. C. Hernandez-Jaramillo, L. Harrison, B. Kelaher, Z. Ristovski and D. P. Harrison, Evaporative cooling does not prevent vertical dispersion of effervescent seawater aerosol for brightening clouds, *Environ. Sci. Technol.*, 2023, **57**, 20559–20570.

27 D. C. Hernandez-Jaramillo, B. Kelaher and D. P. Harrison, A review of plume dispersion and measurement techniques applicable to marine cloud brightening, *Front. Mar. Sci.*, 2025, **12**, 1450175.

28 D. C. Hernandez-Jaramillo, L. Harrison, G. Gunner, A. McGrath, W. Junkermann, W. Lieff, J. Hacker, D. Rosenfeld, B. Kelaher and D. P. Harrison, First generation outdoor marine cloud brightening trial increases aerosol concentration at cloud base height, *Environ. Res. Lett.*, 2025, **20**, 054065.

29 D. C. Hernandez-Jaramillo, C. Medcraft, R. C. Braga, P. Butcherine, A. Doss, B. Kelaher, D. Rosenfeld and D. P. Harrison, New airborne research facility observes sensitivity of cumulus cloud microphysical properties to aerosol regime over the Great Barrier Reef, *Environ. Sci.: Atmos.*, 2024, **4**, 861–871.

30 D. P. Harrison, An overview of environmental engineering methods for reducing coral bleaching stress, *Oceanographic Processes of Coral Reefs*, 2024, pp. 403–418.

31 D. Harrison, M. Baird, L. Harrison, S. Utembe, R. Schofield, R. Escobar Correa, M. Mongin and F. Rizwi, *Environmental Modelling of Large Scale SRM*, Sydney Institute of Marine Science, **https://gbrrestoration.org/rrap-about-us/publications/reports/**, 2019.

32 D. P. Harrison, Z. Ristoviski and M. Gibbs, *Reef Restoration and Adaptation Program: Cooling and Shading*, Australian Institute of Marine Science, Townsville, Australia, 2019.

33 D. Virah-Sawmy, B. Sturmberg and D. P. Harrison, Assessing the availability and feasibility of renewable energy on the Great Barrier Reef-Australia, *Energy Rep.*, 2025, **13**, 2035–2065.

34 K. Alterskjær and J. Kristjánsson, The sign of the radiative forcing from marine cloud brightening depends on both particle size and injection amount, *Geophys. Res. Lett.*, 2013, **40**, 210–215.

35 P. J. Connolly, G. B. McFiggans, R. Wood and A. Tsiamis, Factors determining the most efficient spray distribution for marine cloud brightening, *Philos. Trans. R. Soc., A*, 2014, **372**(2031), 20140056.

36 K. Kawana, Y. Miyazaki, Y. Omori, H. Tanimoto, S. Kagami, K. Suzuki, Y. Yamashita, J. Nishioka, Y. Deng and H. Yai, Number-Size Distribution and CCN Activity of Atmospheric Aerosols in the Western North Pacific During Spring Pre-Bloom Period: Influences of Terrestrial and Marine Sources, *J. Geophys. Res.:Atmos.*, 2022, **127**, e2022JD036690.

37 E. M. Dunne, S. Mikkonen, H. Kokkola and H. Korhonen, A global process-based study of marine CCN trends and variability, *Atmos. Chem. Phys.*, 2014, **14**, 13631–13642.

38 W. C. Hinds and Y. Zhu, *Aerosol technology: Properties, Behavior, and Measurement of Airborne Particles*, John Wiley & Son, 2022.

39 P. Kumar, *Urban ambient aerosol measurements with the DMS500*, Cambustion Application Note, 2009, **https://www.cambustion.com/files/1606395854-dms10v01.pdf**.

40 Y. Wu, Investigation of particle number measurement and combustion and emissions from alternative fuels in diesel engines, Doctoral thesis, The University of Leeds, School of Chemical and Process Engineering, 2019.

41 E. J. Horchler, J. Alroe, L. Harrison, L. Cravigan, D. P. Harrison and Z. D. Ristovski, *Measurement Report: Aerosol and Cloud Nuclei Properties along the Central and Northern Great Barrier Reef: Impact of Continental Emissions*, EGUsphere, 2025, 2025, pp. 1–21.

42 A. Jones, J. Haywood and O. Boucher, A comparison of the climate impacts of geoengineering by stratospheric SO2 injection and by brightening of marine stratocumulus cloud, *Atmos. Sci. Lett.*, 2011, **12**, 176–183.

43 H. Svensmark, M. B. Enghoff, J. Svensmark, I. Thaler and N. J. Shaviv, Supersaturation and critical size of cloud condensation nuclei in marine stratus clouds, *Geophys. Res. Lett.*, 2024, **51**, e2024GL108140.

44 E. Eytan, I. Koren, O. Altaratz, M. Pinsky and A. Khain, Revisiting adiabatic fraction estimations in cumulus clouds: High-resolution simulations with a passive tracer, *Atmos. Chem. Phys.*, 2021, **21**, 16203–16217.

45 A. H. Lefebvre, X. F. Wang and C. A. Martin, Spray characteristics of aerated-liquid pressure atomizers, *J. Propul. Power*, 1988, **4**, 293–298.